X-ray diffraction analysis of lateral composition modulation in InAs/GaSb superlattices intended for infrared detector applications

D.W. Stokes, R.L. Forrest, J.H. Li, S.C. Moss, B.Z. Nosho, B.R. Bennett, L.J. Whitman and M. Goldenberg

Abstract: Lateral compositional modulation in a $(InAs)_{13}/(GaSb)_{13}$ superlattice grown by molecular beam epitaxy for infrared detector applications has been investigated using high-resolution X-ray diffraction. X-ray diffraction reciprocal space maps exhibit distinct lateral satellite peaks about the vertical superlattice peaks; however, the pattern is tilted with respect to the (001) direction. This tilt is directly related to the stacking of the layers as revealed by cross-sectional scanning tunnelling microscopy (XSTM) images. XSTM shows the morphology of the structure to consist of InAs- and GaSb-rich regions with a modulation wavelength of ~ 1200 Å and a lateral composition wavelength of 554 ± 3 Å. The modulation only occurs along one in-plane direction, resulting in InAs 'nanowires' along the $[1\bar{1}0]$ direction, which are several microns long. The possible causes of the lateral composition modulation and its impact on device performance are discussed.

1 Introduction

Detector and laser research based on the InAs/(In)GaSb system has progressed rapidly in recent years but has not reached its full potential due to materials issues. These devices are currently of interest for military applications important for national security, such as chemical sensing and infrared countermeasures against heat-seeking missiles [1–3]. Employing lateral composition modulation (LCM) in the active region of these devices may lead to improved device performance, as has previously been demonstrated in other III–V systems [4, 5]. LCM induces changes in the physical properties of the material (i.e. reduction of bandgap and polarisation anisotropies) and can be characterised by its average composition, average amplitude, wavelength and direction. In general, LCM is avoided in device structures; however, with the recent emergence of nanotechnology, efforts have been made to exploit it for quantum confinement devices such as quantum wire (QWR) based detectors and lasers [6, 7].

LCM refers to the self-assembly of laterally phase-separated, periodic structures perpendicular to the direction of growth of the epitaxial semiconductor films. LCM has been previously observed in a number of materials systems, but has been strongest in short period superlattices (SPSs), e.g. $(GaP)_n/(InP)_m$, and some ternary alloys, e.g. $In_xAl_{1-x}As$, grown by metal organic vapour phase epitaxy (MOVPE) and molecular beam epitaxy (MBE). There are few reports on LCM in InAs/GaSb superlattices [8]; therefore, for the system's potential to be realised, a detailed analysis of the structural properties is necessary.

In this paper, we present the results of the X-ray diffraction analysis of LCM in an InAs/GaSb superlattice intended for infrared detector applications. The average morphology of the structure, i.e. the vertical and lateral modulation wavelengths, the strain in the layers, and the orientation of the LCM will be described. The possible causes of the LCM and the impact of LCM on device performance will be addressed.

2 Experimental details

The detector structure consists of a $(InAs)_{13}/(GaSb)_{13}$ superlattice (SL) grown on a (001) GaSb substrate in a solid source molecular beam epitaxy (MBE) system at the Naval Research Laboratory. Following deposition of the buffer layer a 140 period SL was grown at 390°C. Migration-enhanced epitaxy (MEE) was used to obtain InSb bonds at the interfaces where the interfacial bond characteristics can affect the properties of the material, i.e. carrier concentration and bandgap [9, 10]. The first 90 periods were p-type $(InAs)_{13}/(GaSb)_{13}$ (Be doped) and the last 50 periods were n-type (Si doped InAs). Because Si is a p-type dopant in GaSb, only the InAs layers were doped within the n-type section of the superlattice. Further details of the growth are given elsewhere [11]. The superlattice period was 80 Å with each bilayer having a nominal thickness of 40 Å.

High-resolution X-ray diffraction (XRD) radial scans and reciprocal space maps were taken on a four-circle diffractometer using Cu K_{α_1} radiation ($\lambda = 1.54041$ Å) from a 12 kW rotating anode. Cross-sectional scanning

IEE Proceedings online no. 20030643

doi: 10.1049/ip-opt:20030643

Paper received 15th October 2002

D.W. Stokes, J.H. Li and S.C. Moss are with the Department of Physics, University of Houston, Houston, TX 77204, USA

R.L. Forrest was with the Department of Physics, University of Houston and is now with the University of Houston-Downtown, Department of Natural Sciences, Houston, TX 77002, USA

B.Z. Nosho was with the Naval Research Laboratory and is now with the HRL Laboratories, LLC, Malibu, CA 90265, USA

B.R. Bennett and L.J. Whitman are with the Naval Research Laboratory, Washington, DC 20375, USA

M. Goldenberg is with SFA, Inc., Largo, MD 20774, USA

Report Documentation Page

Form Approved
OMB No. 0704-0188

1. REPORT DATE	2. REPORT TYPE	3. DATES COVERED
OCT 2002		**00-00-2002 to 00-00-2002**

4. TITLE AND SUBTITLE	5a. CONTRACT NUMBER
X-ray diffraction analysis of lateral composition modulation in InAs/GaSb superlattices intended for infrared detector applications	5b. GRANT NUMBER
	5c. PROGRAM ELEMENT NUMBER
6. AUTHOR(S)	5d. PROJECT NUMBER
	5e. TASK NUMBER
	5f. WORK UNIT NUMBER
7. PERFORMING ORGANIZATION NAME(S) AND ADDRESS(ES) **Naval Research Laboratory,Plasma Physics Division,4555 Overlook Avenue SW,Washington,DC,20375**	8. PERFORMING ORGANIZATION REPORT NUMBER
9. SPONSORING/MONITORING AGENCY NAME(S) AND ADDRESS(ES)	10. SPONSOR/MONITOR'S ACRONYM(S)
	11. SPONSOR/MONITOR'S REPORT NUMBER(S)

12. DISTRIBUTION/AVAILABILITY STATEMENT
Approved for public release; distribution unlimited

13. SUPPLEMENTARY NOTES

14. ABSTRACT
see report

15. SUBJECT TERMS

16. SECURITY CLASSIFICATION OF:			17. LIMITATION OF ABSTRACT	18. NUMBER OF PAGES	19a. NAME OF RESPONSIBLE PERSON
a. REPORT **unclassified**	b. ABSTRACT **unclassified**	c. THIS PAGE **unclassified**	**Same as Report (SAR)**	**4**	

tunnelling microscopy (XSTM) images of the modulated structures were obtained following cleavage in ultra-high vacuum as previously described [12].

3 Results

The morphology of the structure is demonstrated in the XSTM image of a (110) cleavage surface through the superlattice, Fig. 1. Lateral thickness undulations are clearly seen in both the InAs and GaSb layers, dark and light regions along the (110) surface, respectively, but are more prominent in the InAs layers. This morphology is unconventional when compared to the structure predicted for LCM formation during SPS growth where the layers stack out-of-phase [13], Fig. 2*a*. In this mode, layers A and B stack 180° out-of-phase and have equal and opposite strain. Elastic instability theory predicts that material B prefers to grow on the troughs of material A due to the stress/strain state resulting from the underlying interface [13]. For this sample, the stacking is a result of the fact that the InAs layers undulate more than the GaSb and that the GaSb prefers to grow in between the trough and crest of the InAs layer rather than on the trough. Each sequential layer stacks 90° out-of-phase (Fig. 2*b*) and the layers are alternately under compressive (InAs) and tensile strain (GaSb). The larger-scale light and dark regions along the growth direction are an artefact of the alternately enriched, GaSb- and InAs-rich regions, respectively. The contrast in the image occurs due to relaxation in the layer as a result of the different strain states of the two regions.

XRD reciprocal space maps (RSMs) about the (004) Bragg peaks in the plane perpendicular to the lateral modulations ($\phi \equiv 0°$) and in the plane parallel to (containing) the LCM ($\phi \equiv 90°$) are shown in Fig. 3. The ($\bar{4}\bar{4}4$) RSMs with $\phi \equiv 0°$ and $\phi \equiv 90°$, not shown, indicate that the superlattice is fully strained to the GaSb substrate and buffer since the average superlattice (SL0) peaks and GaSb peak are aligned along the [001] direction. The vertical SL wavelength was $\Lambda_{SL} = 155 \pm 10$ Å where the intended SL wavelength was 80 Å. The doubling of the intended wavelength corresponds to the stacking of the LCM layers and the ± 10 Å variation of Λ_{SL} is due to splitting in the satellite peaks.

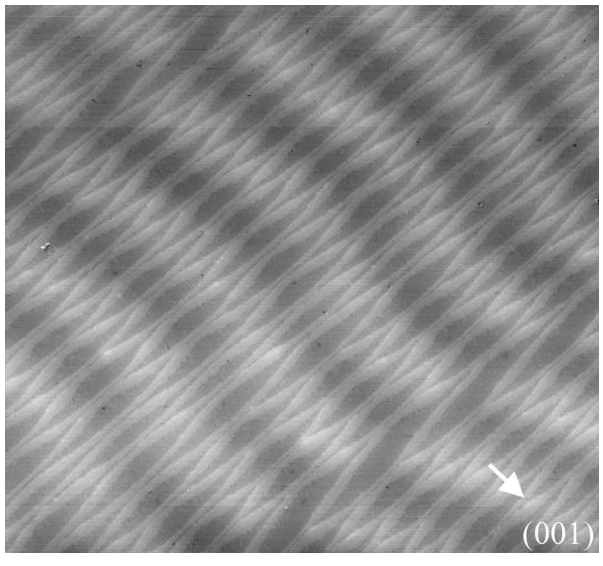

Fig. 1 *XSTM image of LCM in 140-period* $(InAs)_{13}/(GaSb)_{13}$ *superlattice*

Bright and dark layers correspond to GaSb and InAs, respectively, on a (110) cross-sectional surface

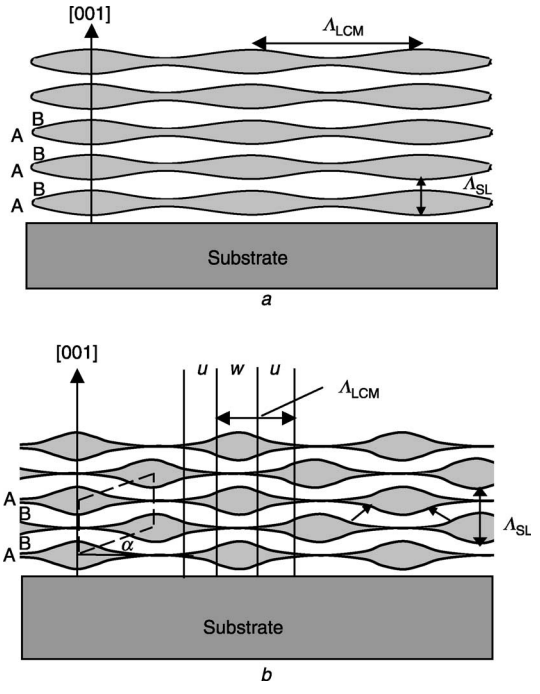

Fig. 2 *Schematic diagrams of out-of-phase stacking for LCM*

a Predicted 180° out-of-phase stacking for LCM in SPS
b 90° out-of-phase stacking observed for LCM in 140-period $(InAs)_{13}/(GaSb)_{13}$ superlattice. Small arrows indicate where Ga(As)Sb layer is thickest

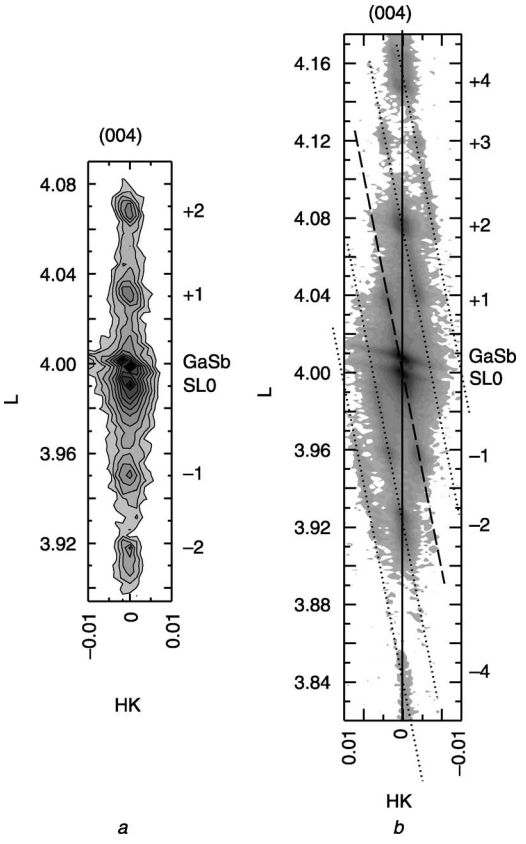

Fig. 3 *XRD reciprocal space map of LCM in 140 period InAs/GaSb superlattice about (004) Bragg peak with* $\Phi = 0°$ *(a) and* $\Phi = 90°$ *(b)*

Both the vertical and lateral peaks are tilted from the (001) plane (solid line) by $7.5 \pm 0.5°$ and are indicated by the dashed line (vertical satellite peaks) and the dotted line (lateral peaks)

The RSMs taken with $\phi = 90°$ confirmed the presence of LCM, with both vertical and lateral satellite peaks observed. However, the vertical peaks are tilted from the (001) direction by $7.5 \pm 0.5°$ as indicated by the solid line along (001). The dashed lines contain the vertical satellite peaks and the dotted lines contain the lateral peaks. The LCM wavelength measured from the RSMs is $\Lambda_{LCM_o} = 554 \pm 3$ Å, which is in excellent agreement with the 600 Å spacing measured between the bright (or dark) bands in the XSTM image.

The average SL lattice constants determined from all of the scans are $a = 6.0959$ Å (in-plane), and $c = 6.1080 \pm 0.001$ Å (out-of-plane), where GaSb was assumed to be relaxed ($a = 6.0959$ Å). The out-of-plane lattice constant is larger than that of GaSb and InAs, which indicates that there is some alloying in the layers [11].

4 Discussion

From simulations of the XRD data, the average vertical and lateral modulation wavelengths, layer thickness variations and superlattice lattice constant were determined. The strain/stress state and orientation of the LCM were also determined. The average vertical period, $\Lambda_{SL} = 155 \pm 10$ Å, is twice the intended period, 80 Å due to the unusual stacking of the modulated layers. The ± 10 Å variation in Λ_{SL} is due to a splitting in the satellite peaks, which indicates that there are two or more discrete superlattice periods formed along the growth direction. This was evident in the XSTM images taken of the entire vertical height of the structure [14] (not shown), where the undulations did not become regular until after about 40 periods, and became irregular after 80 periods. The lateral wavelength, $\Lambda_{LCM} = 554 \pm 3$ Å, is similar in magnitude to the 100 to 400 Å wavelengths reported for other LCM systems, where it is generally found that the lateral and undulating wavelengths are identical; however, this is not the case for this sample. The undulation wavelength was 1200 Å (measured from Fig. 1 assuming a sinusoidal undulation). The layer thickness undulations varied from 4–28 ML in the InAs(Sb) layers and from 8–18 ML in the Ga(As)Sb layers.

The tilt of the XRD pattern is directly related to the stacking of the layers, which can be seen in Fig. 2*a*. The parallelogram shown represents a unit cell of the superstructure; that is, a cell containing one vertical and lateral period. The base of the unit cell is tilted by an angle α with respect to the [110] direction. This angle is related to the lateral and vertical periods by $\tan^{-1}((1/2\Lambda_{SL})/\Lambda_{LCM})$, yielding an angle of 7.96°, which is in excellent agreement with the angle determine from the tilt of the XRD pattern away from the (001) plane.

The XRD RSM is similar to those from LCM structures grown on intentionally miscut substrates, in which the tilt angle is equal to the miscut angle [15, 16]. This is not true for this sample, which was grown on a nominally (001) substrate. X-ray measurements indicate a miscut of less than 0.2°. Although this is quite small, it will introduce lateral steps on the surface [17, 18], which may result in the preferred stacking direction observed.

The in-plane lattice constant indicates that the superlattice is fully strained to the GaSb substrate and buffer. The out-of-plane lattice constant (6.1080 Å) indicates that alloying occurs in the layers. There is less than 4% As in the GaSb layers and ~8% Sb in the InAs layers of the InAs-rich regions and ~12% Sb in the InAs layers in the GaSb-rich regions. Numerous studies have been performed on alloying in InAs/GaSb superlattices due to incorporation during growth, interdiffusion at the interfaces and cross-contamination [19–21]. Alloying in the layers, in particular, the InAs(Sb) layer, increases the strain state of the layer; therefore, this will affect the lateral modulation wavelength. Generally, in InAs/GaSb superlattices grown on GaSb substrates, the GaSb layer is unstrained while the InAs layer is under tensile strain due to its smaller lattice constant. However, with alloying, now the InAs(Sb) and Ga(As)Sb layers are under compressive and tensile strain, respectively. It has been observed that compressive strain is more likely to lead to film instabilities [22–24]; therefore, this may explain why the InAs(Sb) layers undulate more than the Ga(As)Sb layers. Alloying in the layers also affects the surface tension of the InAs layers. With the occurrence of alloying, the InAs(Sb) surface tension, which is smaller than that of GaSb, is reduced while that of Ga(As)Sb is increased, making it more likely to form undulations. We believe that strain, surface tension or a combination of these affects may be responsible for the larger thickness variation in the InAs(Sb) layer [13, 25–30].

It is unclear as to why the Ga(As)Sb prefers to grow between a crest and a trough of the InAs layers. We believe that this may be explained by GaSb growth on facetted surfaces. It has been shown that the growth rate of GaSb (by metalorganic molecular beam epitaxy) is enhanced on (11n) substrates over that on (001) [31]. This may imply that the growth rates will also be enhanced at atomic steps consisting of (11n) planes. Although this sample was grown on a nominally (001) substrate, XRD indicates a 0.2° miscut. Even this small miscut will introduce steps on the surface; therefore, the GaSb may grow at a faster rate on the step edges of the InAs layer, resulting in the observed stacking of the layers.

The modulation observed is only along one in-plane direction, [110], and results in the formation of InAs 'nanowires' several micrometres in length, along the $[1\bar{1}0]$ direction as seen in the atomic force microscopy (AFM) image of the (001) growth surface in Fig. 4. These naturally formed 'nanowires' may be useful for quantum wire (QWR) applications, such as detectors, lasers and light-emitting diodes. In order for LCM structures to be useful as devices, the modulation must be highly uniform, equal in size and shape, the material must have a low defect density and the LCM must be small for observation of zero-dimensional confinement effects. The difficulty with LCM structures lies with the ability to reproduce the structure, which poses an additional barrier for a system that is known to have materials issues. A preliminary growth study was performed to address the question of how the LCM or wire formation is affected by changes in layer thickness, buffer layer and substrate choice [8]. Thicker GaSb layers lead to a longer undulation wavelength while an AlSb buffer layer on a GaSb substrate leads to shorter undulation wavelengths. For growth on an InAs buffer and substrate no undulations

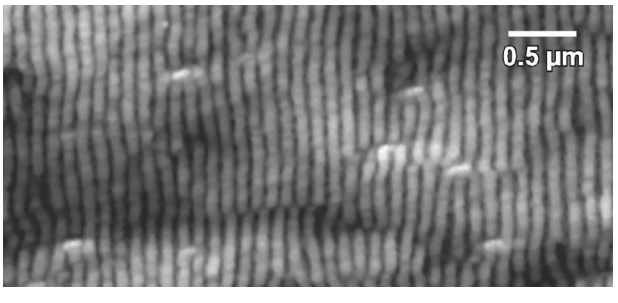

Fig. 4 *AFM image of the (001) growth surface of the $(InAs)_{13}/(GaSb)_{13}$ superlattice structure showing nanowires, several microns in length, along the $[1\bar{1}0]$ direction*

were observed. However, this sample was also grown with GaAs interfacial bonds; therefore, a direct comparison of the structures cannot be made. From this growth study, it is clear that strain, due to interfacial bonds, i.e. InSb versus GaAs, surface tension, and lattice mismatch, play a major role in the undulation formation. By carefully controlling the strain state of the layers, LCM formation may be controlled making it appealing for device applications.

The impact of LCM on device performance is the subject of ongoing investigations. The combination of the internal effects of the strain and LCM will alter the energy gap of the superlattice for a given layer thickness, which is critical for utilising these structures in the active regions of devices.

5 Acknowledgments

The authors would like to thank W. Donner for valuable discussions concerning XRD data analysis. Research at the University of Houston was supported by the National Science Foundation on DMR-0099573, the Texas Center for Superconductivity and Advanced Materials (TcSAM) through the state of Texas and the University of Houston New Faculty Research Program. Research at Naval Research Laboratory was supported by the Office of Naval Research and the Defense Advanced Research Program Agency.

6 References

1 Choi, H.K.: 'Mid-infrared semiconductor lasers', *Rev. Laser Eng.*, 1997, **25**, p. 14
2 Stokes, D.W., Olafsen, L.J., Bewley, W.W., Vurgaftman, I., Felix, C.L., Aifer, E.H., Meyer, J.R., and Yang, M.J.: 'Type-II' "W" lasers emitting at $\lambda = 5.4-7.3$ μm', *J. Appl. Phys.*, 1999, **86**, (9), pp. 4729–4733
3 Bewley, W.W., Lee, H., Vurgaftman, I., Menna, R.J., Felix, C.L., Martinelli, R.U., Stokes, D.W., Garbuzov, D.Z., Meyer, J.R., Maiorov, M., Conolly, J.C., Sugg, A.R., and Olsen, G.H.: 'Continuous-wave operation of $\lambda = 3.25$ mm broadened waveguide 'W' quantum-well diode lasers up to T = 195 K', *Appl. Phys. Lett.*, 2000, **76**, (3), pp. 256–258
4 Arakawa, Y., and Sakaki, H.: 'Multidimensional quantum well laser and temperature dependence of its threshold current', *Appl. Phys. Lett.*, 1982, **40**, pp. 939–941
5 Yariv, A.: 'Scaling laws and minimum threshold currents for quantum confined semiconductor lasers', *Appl. Phys. Lett.*, 1988, **53**, pp. 1033–1035
6 Chou, S.T., Cheng, K.Y., Chou, L.J., and Hsieh, K.C.: '$Ga_xIn_{1-x}As$ quantum wire lasers grown by strained-induced lateral-layer ordering process', *Appl. Phys. Lett.*, 1995, **66**, (17), pp. 2220–2222
7 Wohlert, D.E., Cheng, K.Y., and Chou, S.T.: 'Temperature invariant lasing and gain spectra in self-assembled GaInAs quantum wire Fabry–Perot lasers', *Appl. Phys. Lett.*, 2001, **78**, (8), pp. 1047–1049
8 Nosho, B.Z., Bennett, B.R., Whitman, L.J., and Goldenberg, M.: 'Spontaneous growth of an InAs nanowire lattice in an InAs/GaSb superlattice', *Appl. Phys. Lett.*, 2002, **81**, pp. 4452–4454
9 Chow, D.H., Miles, R.H., Soderstrom, J.R., and McGill, T.C.: 'Growth and characterization of $InAs/Ga_{1-x}$ In_xSb strained layer superlattices', *Appl. Phys. Lett.*, 1990, **56**, pp. 1418–1420
10 Chow, D.H., Miles, R.H., and Hunter, A.T.: 'Effects of interface stoichiometry on the structural and electronic properties of $Ga_{1-x}In_xSb/InAs$ superlattices', *J. Vac. Sci. Technol. B, Microelectron. Process. Phenom.*, 1992, **10**, (2), pp. 888–891
11 Nosho, B.Z., Bennett, B.R., Whitman, L.J., and Goldenberg, M.: 'Effects of As_2 versus As_4 on InAs/GaSb heterostructures: As-for-Sb exchange and film stability', *J. Vac. Sci. Technol. B, Microelectron. Nanometer Struct.*, 2001, **19**, (4), pp. 1626–1630
12 Nosho, B.Z., Barvosa-Carter, W., Yang, M.J., Bennett, B.R., and Whitman, L.J.: 'Interpreting interfacial structure in cross-sectional STM images of III–V semiconductor heterostructures', *Surf. Sci.*, 2000, **465**, pp. 361–371
13 Shilkrot, L.E., Srolovitz, D.J., and Tersoff, J.: 'Morphology evolution during the growth of strained-layer superlattices', *Phys. Rev. B, Condens. Matter*, 2000, **62**, (12), pp. 8397–8409
14 Stokes, D.W., Forrest, R.L., Li, J.H., Moss, S.C., Nosho, B.Z., Bennett, B.R., Whitman, L.J., and Goldenberg, M.: 'Lateral composition modulation in InAs/GaSb superlattices', *J. Appl. Phys.*, 2002, **93**, pp. 311–315
15 Holy, V., Pietsch, U., and Baumbach, T.: 'High-resolution X-ray scattering from thin films and multilayers' (Springer, Berlin, 1999)
16 Giannini, C., Baumbach, T., Lubbert, D., Felici, R., Tapfer, L., Marschner, T., Stolz, W., Jin-Phillipp, N.Y., and Phillipp, F.: 'Strain-driven transitions from stepped interfaces to regularly spaced macro-steps in (GaIn)As/Ga(PAs) symmetrically strained superlattices', *Phys. Rev. B, Condens. Matter*, 2000, **61**, (3), pp. 2173–2179
17 Marschner, T., Lutgen, S., Volk, M., Stolz, W., and Gobel, E.O.: 'Investigations of the structural stability of highly strained [(Al)GaIn]As/Ga (PAs) multiple quantum wells', *Appl. Phys. Lett.*, 1996, **69**, (15), pp. 2249–2251
18 Giannini, C., Tapfer, L., Zhang, Y., De Caro, L., Marschner, T., and Stolz, W.: 'Structural ordering and interface morphology in symmetrically strained (GaIn)As/Ga(PAs) superlattices grown on off-oriented GaAs (100)', *Phys. Rev. B, Condens. Matter*, 1997, **55**, (8), pp. 5276–5283
19 Fenstra, R.M., Collins, D.A., Ting, D.Z.-Y., and Wang, M.W.: 'Interface roughness and asymmetry in InAs/GaSb superlattices studied by scanning tunneling microscopy', *Phys. Rev. Lett.*, 1994, **72**, (17), pp. 2749–2752
20 Magri, R., and Zunger, A.: 'Effects of interfacial atomic segregation and intermixing on the electronic properties of InAs/GaSb superlattices', *Phys. Rev. B, Condens. Matter Mater. Phys.*, 2002, **65**, pp. 165302
21 Harper, J., Weimer, M., Zhang, D., Lin, C.-H., and Pei, S.S.: 'Microstructure of the GaSb-on-InAs heterojunction examined with cross-sectional scanning tunneling microscopy', *Appl. Phys. Lett.*, 1998, **73**, (19), pp. 2805–2807
22 Xie, Y.H., Gilmer, G.H., Roland, C., Silverman, P.J., Buratto, S.K., Cheng, J.Y., Fitzgerald, E.A., Kortan, A.R., Schuppler, S., Marcus, M.A., and Citrin, P.H.: 'Semiconductor surface roughness: dependence on sign and magnitude of bulk strain', *Phys. Rev. Lett.*, 1994, **73**, (22), pp. 3006–3009
23 Tersoff, J.: 'Step energies and roughening of strained layers [comment]', *Phys. Rev. Lett.*, 1995, **74**, (24), p. 4962
24 Xie, Y.H., Gilmer, G.H., Roland, C., Silverman, P.J., Buratto, S.K., Cheng, J.Y., Fitzgerald, E.A., Kortan, A.R., Schuppler, S., Marcus, M.A., and Citrin, P.H.: 'Step energies and roughening of strained layers [Reply to comment]', *Phys. Rev. Lett.*, 1995, **74**, (22), p. 4963
25 Srolovitz, D.J.: 'On the stability of surfaces of stressed solids', *Acta Metall.*, 1989, **37**, (2), pp. 621–625
26 Spencer, B.J., Voorhees, P.W., and Davis, S.H.: 'Morphological instability in epitaxially strained dislocation-free solid films: linear stability theory', *J. Appl. Phys.*, 1993, **73**, (10), pp. 4955–4970
27 Shilkrot, L., Srolovitz, D.J., and Tersoff, J.: 'Dynamically stable growth of strained-layered superlattices', *App. Phys. Lett.*, 2000, **77**, (2), pp. 304–306
28 Spencer, B.J., Davis, S.H., and Voorhees, P.W.: 'Morphological instability in epitaxially strained dislocation-free solid films: Nonlinear evolution', *Phys. Rev. B, Condens. Matter*, 1993, **47**, (15), pp. 9760–9777
29 Guyer, J.E., and Voorhees, P.W.: 'Morphological stability and compositional uniformity of alloy thin films', *J. Cryst. Growth*, 1998, **187**, pp. 150–165
30 Spencer, B.J., Voorhees, P.W., and Tersoff, J.: 'Morphological instability theory for strained alloy film growth: the effect of compositional stresses and species-dependent surface mobilities on ripple formation during epitaxial film deposition', *Phys. Rev. B, Condens. Matter. Mater. Phys.*, 2001, **64**, (15), pp. 235318/1–31
31 Yamamoto, K., Asahi, H., Hidaka, K., Satoh, J., and Gonda, S.: 'Growth rate enhancement of III–V antimonides on high-index substrates in metalorganic molecular beam epitaxy', *J. Cryst. Growth*, 1997, **179**, pp. 37–40